Title: Auranofin inhibits virulence in *Pseudomonas aeruginosa*

Authors: Leon Zhen Wei Tan[1,2,6], Joey Kuok Hoong Yam[2,6], Ziyan Hong[2,6], May Margarette Santillan Salido[2], Bau Yi Woo[1,2], Sam Fong Yau Li[1], Liang Yang[2,3,5], Michael Givskov[2,4*], Shu-Sin Chng[1,2,7*]

Affiliations:

[1]Department of Chemistry, National University of Singapore, Singapore 117543.

[2]Singapore Center for Environmental Life Sciences Engineering (SCELSE), Singapore.

[3]School of Biological Sciences, Nanyang Technological University, Singapore 639798, Singapore

[4]Costerton Biofilm Center, Department of Immunology and Microbiology, University of Copenhagen, DK- 2200, Denmark

[5]Present address: School of Medicine, Southern University of Science and Technology, Shenzhen 518055, Guangdong Province, China

[6]These authors contributed equally to this work

[7]Lead contact

[*]To whom correspondence should be addressed.

E-mail: (S.-S.C) chmchngs@nus.edu.sg, (M.G) mgivskov@sund.ku.dk

Abstract

Pseudomonas aeruginosa is widely attributed as the leading cause of hospital-acquired infections. Due to intrinsic antibiotic resistance mechanisms and the ability to form biofilms, *P. aeruginosa* infections are challenging to treat. *P. aeruginosa* employs multiple virulence mechanisms to establish infections, many of which are controlled by the global virulence regulator Vfr. An attractive strategy to combat *P. aeruginosa* infections is thus the use of anti-virulence compounds. Here, we report the discovery that FDA-approved drug auranofin attenuates virulence in *P. aeruginosa*. We demonstrate that auranofin acts by targeting Vfr, which in turn leads to inhibition of quorum sensing (QS) and Type IV pili (TFP). Consistent with inhibition of QS and TFP expression, we show that auranofin attenuates biofilm maturation, and when used in combination with colistin, displays strong synergy in eradicating *P. aeruginosa* biofilms. Auranofin may have immediate applications as an anti-virulence drug against *P. aeruginosa* infections.

Introduction

Pseudomonas aeruginosa is a prevalent opportunistic pathogen known for its potent virulence, environmental versatility and multi-drug resistance. Its role as the leading cause of hospital-acquired infections (HAIs) among immuno-compromised patients is well documented[1]. Notably, it is one of the main causes of pneumonia in cystic fibrosis (CF) patients[2], and wound infections in surgical patients or burn victims[3]. Furthermore, *P. aeruginosa* has been known to thrive in a variety of ecological niches[4], allowing colonization on abiotic surfaces like catheters and other implanted medical devices[5,6]. Increasing incidences of multi-drug resistant (MDR) *P. aeruginosa* infections[7,8] in the clinic pose a serious threat to global health, underscoring the need to develop new strategies to combat these pathogens.

P. aeruginosa carries several intrinsic antibiotic resistance mechanisms involving the collaboration of restricted uptake through the outer membrane[9], the use of energy-dependent efflux pumps[10,11], and expression of β-lactamases[12,13]. In addition, *P. aeruginosa*, like many other bacteria, exhibits a form of social behavior known as biofilm formation[14], which further increases its tolerance to antibiotics[15]. A biofilm is a community of bacteria encased in a polymeric mesh consisting of extracellular DNA (eDNA), proteins and polysaccharides. In the clinic, significantly higher patient mortality has been associated with the formation of biofilms in the lungs of CF patients[16]. Specifically, the presence of biofilms increases the complexity of treatment due to the function of the extracellular matrix as a physical barrier against, and sponge for, antimicrobial drugs[15]. The small pore size of the biofilm mesh effectively reduces penetration of lysozymes and macromolecular drugs, presumably decreasing the immediate concentrations of these agents surrounding the cells. Additionally, the biofilm matrix is also highly negatively charged due to the presence of eDNA and polysaccharides, which protect the colony from positively-charged aminoglycosides[17]. Consequently, the inhibition of biofilm

58 formation, maturation and/or function remains a principal consideration in the search for new
59 treatment options against *P. aeruginosa*.

60 An attractive alternative strategy to control bacterial infections has been the use of small
61 molecules that block virulence. Such anti-virulence compounds may reduce the ability of
62 bacteria to infect the host[18,19], and/or attenuate bacterial defenses against host immune cells[20],
63 thereby facilitating clearance of the infection site[21]. The virulence of *P. aeruginosa* is multi-
64 faceted but largely controlled by the global virulence factor regulator, Vfr[22]. Vfr is a cyclic
65 adenosine monophosphate (cAMP)-dependent transcription factor that coordinates expression
66 of roughly 200 genes[23,24]. It regulates virulence directly by activating expression of secretion
67 systems[25] (e.g. Type III) and the pilus formation machinery[26] (Type IV). The Type III secretion
68 system (T3SS) in *P. aeruginosa* mediates cytotoxicity against host cells through the delivery
69 of molecular effectors that can disrupt host processes[27]. The Type IV Pilus (TFP) is important
70 for twitching motility[28], and often associated with the establishment and maturation of *P.*
71 *aeruginosa* biofilms. Vfr also controls quorum sensing (QS)[29], a cell-cell communication
72 network involving the *las*-, *rhl*- and *pqs*-encoded systems, which plays a role in the production
73 of several virulence factors including extracellular proteases, biosurfactants and toxins[20], and
74 is important for biofilm maturation[30] and immune evasion. While many small molecules that
75 inhibit QS and T3SS have been reported[31-33], no inhibitors of Vfr and TFP have been
76 discovered to date.

77 In this work, we identified auranofin, an FDA-approved, gold(I)-based anti-
78 inflammatory drug, as a potent inhibitor of virulence in *P. aeruginosa*. We show that auranofin
79 inhibits QS and TFP formation at low micromolar concentrations. It does this in part by
80 targeting cysteines in Vfr and abolishing the ability of Vfr to bind DNA. Using flow cell biofilm
81 assays, we demonstrate that auranofin is able to attenuate biofilm maturation. Furthermore,
82 auranofin displays strong synergistic effects in eradicating *P. aeruginosa* biofilms *in vitro*,

83 when used in combination with colistin. This synergy is also observed in a murine infection
84 model. We propose that auranofin can potentially be re-purposed as an anti-virulent drug to
85 treat *P. aeruginosa* infections.

86 **Results**

87 **Auranofin inhibits QS in *Pseudomonas aeruginosa***

88 We initially discovered auranofin in a screen to identify small molecules that inhibit
89 QS in *P. aeruginosa*. We screened ~6,000 compounds from various libraries using a *lasB-*
90 *gfp*(ASV) strain[34], where expression of a fusion construct between LasB N-terminus and an
91 unstable GFP variant (GFP(ASV)) is controlled by constitutively expressed LasR, the cognate
92 transcriptional regulator of the *las* pathway. Inhibitors of this pathway should reduce GFP
93 fluorescence in this assay. In addition, since the *las* pathway controls both the *rhl* and *pqs*
94 pathways, compounds identified in this screen could potentially shut down the entire QS
95 network. We found that auranofin exhibits sub-micromolar (IC_{50}) inhibition of LasB-GFP
96 expression with minimal effects on cell growth (Fig. 1A and S1). Auranofin also strongly
97 inhibits fluorescence in two other reporter strains, *rhlA-gfp*(ASV) and *pqsA-gfp*(ASV)[35], both
98 under the control of their respective transcriptional activators, RhlR and PqsR (Fig. 1B and
99 1C). To validate our findings, we examined the effects of auranofin on the levels of RNA
100 transcripts for key QS-regulated genes, as well as on the production of various QS-controlled
101 virulence factors. Auranofin results in the down-regulation of *lasA* and *rhlA* transcripts (Fig.
102 S2), and significantly reduces the levels of elastase (LasB), rhamnolipids and pyocyanin (Fig.
103 2). Taken together, these results establish that auranofin is a potent QS inhibitor.

104

105 **Auranofin inhibits expression of Type IV pili (TFP), and likely Type III secretion system**
106 **(T3SS), in *P. aeruginosa***

107 To gain insights into the mechanism(s)-of-action of auranofin, we compared the protein
108 profiles of *P. aeruginosa* in the presence and absence of auranofin. Proteomic analysis showed
109 that about 210 proteins were significantly up- or down-regulated in the presence of auranofin.
110 Several efflux pumps were the most up-regulated, while certain outer membrane porins were

111 down-regulated in the presence of auranofin (Table S1). These changes indicate a response to
112 prevent intracellular build-up of auranofin. Notably, consistent with it being a QS inhibitor,
113 treatment with auranofin caused reduction in the levels of proteins involved in or regulated by
114 QS. Interestingly, we also observed down-regulation of proteins involved in T3SS and TFP
115 formation. We showed that auranofin is able to inhibit TFP-dependent motility, including
116 swarming and twitching[36,37] (Fig. 3). Our observations here are, in part, due to transcriptional
117 down-regulation of these systems (Fig. S2). These results imply that auranofin either has
118 multiple targets, and/or it targets a transcriptional regulator upstream of QS, T3SS and TFP.
119

120 **Auranofin inhibits Vfr *in vitro* but has other targets in cells**

121 QS, T3SS and TFP formation are positively regulated by Vfr[24]. We asked if auranofin
122 directly targets Vfr function. To test this, we examined the ability of auranofin to inhibit the
123 function of Vfr in binding to promoter sequences *in vitro* using electrophoretic mobility shift
124 assays (EMSA). We first showed that purified Vfr is able to specifically bind DNA fragments
125 containing the promoter region of *lasR*, a representative QS gene (Fig. S3), as previously
126 reported[38]. We further demonstrated that auranofin effectively prevents Vfr binding to this
127 promoter in a dose-dependent manner, indicating that it inhibits Vfr function *in vitro* (Fig. 4A).
128 Gold(I)-based compounds are thiophilic, and auranofin has previously been shown to react
129 covalently with cysteine residues within target proteins[39,40]. To ascertain if its inhibition of Vfr
130 proceeded via covalent modification of cysteines, we generated a cysteine-less Vfr variant
131 (VfrΔ5) in which all five cysteines were replaced by serine residues. This variant is functional
132 as judged by its ability to bind the *lasR* promoter *in vitro* (Fig. S3). Remarkably, auranofin is
133 no longer able to prevent binding of VfrΔ5 to this promoter (Fig. 4B). These results establish
134 that auranofin inhibits Vfr *in vitro* via its cysteine residues.

135 To determine if Vfr is the main target of auranofin in cells, we complemented the Δ*vfr*
136 strain with wild-type Vfr and the VfrΔ5 variant, and examined the elastase levels and twitching
137 motility in the presence and absence of auranofin. Both wild-type Vfr and the VfrΔ5 variants
138 were able to complement the Δ*vfr* strain in these assays (Fig. S4). We showed that auranofin
139 inhibits both phenotypes in the wild-type Vfr complemented strain, as expected. Surprisingly,
140 auranofin was still able to inhibit these phenotypes in the VfrΔ5 complemented strain, unlike
141 what we have observed *in vitro*. While we have demonstrated that auranofin does inhibit Vfr
142 via its cysteine residues *in vitro*, our data suggests auranofin may have other targets, in addition
143 to Vfr.
144
145 **Auranofin impedes the development of *P. aeruginosa* biofilms**
146 Both TFP and QS are required during biofilm development[41,42]. TFP are important for
147 initial surface attachment of cells, as well as for the organization of cells into the typical
148 "mushroom" architecture of mature *P. aeruginosa* biofilms. QS is also critical for biofilm
149 maturation, although the mechanisms here are less understood. Since auranofin inhibits both
150 TFP formation and QS networks, we expect it to also have an impact on the development of *P.*
151 *aeruginosa* biofilms. To test this, we monitored biofilm formation and maturation in the
152 presence and absence of auranofin over a period of 72 h in continuous flow chambers, using
153 Δ*lasI*Δ*rhlI* as the control strain. The formation of fully matured, canonical mushroom-shaped
154 biofilm structures for wild-type *P. aeruginosa* was readily observed within 48 h (Fig. 5A).
155 Interestingly, while auranofin did not have obvious effects on the initial surface attachment of
156 cells at early time points (6 h and 24 h), it impeded the development of mushroom-shaped
157 structures beyond 48 h, and only allowed formation of microcolonies. Biofilms formed in the
158 presence of auranofin appeared flatter, similar to biofilms of QS-null (e.g. Δ*lasI*Δ*rhlI*) and/or
159 TFP-null strains[43]. Detailed analyses of these biofilms revealed that biomass (Fig. 5B), mean

160 biomass thickness (Fig. 5C), and the roughness coefficient (Fig. 5D) were all significantly
161 reduced in the presence of auranofin after 48 h. Our data clearly indicate that despite permitting
162 biofilm attachment and growth, auranofin attenuates the progression of biofilm maturation,
163 likely by inhibiting QS and TFP.
164

165 **Auranofin exhibits synergistic effects with colistin in killing *P. aeruginosa* biofilms**

166 Since auranofin affects the maturation of the biofilm, we asked whether it may display
167 synergy with colistin, a last resort drug commonly used to treat *P. aeruginosa* infections. We
168 first evaluated the combined effects of auranofin and colistin by monitoring viability of *P.*
169 *aeruginosa* cells, following treatment of biofilms (pre-formed for one day on glass beads) with
170 different concentrations of the two drugs in a checkerboard format. The highest concentrations
171 of auranofin (10 μM) or colistin (10 μg ml^{-1}) single treatment only reduced the average number
172 of viable bacterial cells per glass bead from ~1 x 10^7 c.f.u. (no treatment) to ~3.1 x 10^6 c.f.u.
173 or ~5.7 x 10^6 c.f.u., respectively (Fig. 6A). Remarkably, the number of viable bacterial cells
174 was drastically reduced (average ~178 c.f.u./glass bead) when the biofilms were treated with a
175 combination of lower concentrations of auranofin (2 μM) and colistin (2 μg ml^{-1}),
176 demonstrating strong synergistic effects. We also tested the synergy of auranofin and colistin
177 using *P. aeruginosa* flow cell biofilms. As previously reported, colistin treatment alone (at 10
178 μg ml^{-1}) resulted in a sharp decline in cell viability across a 2-day old biofilm, with the
179 exception of several surviving colistin-tolerant subpopulations[43] (Fig. 6B). Interestingly,
180 adding auranofin (1 μM) prior to biofilm formation allowed subsequent colistin treatment to
181 completely eradicate the *P. aeruginosa* biofilm. In addition, co-treatment of a 2-day biofilm
182 with auranofin and colistin also resulted in complete killing. Taken together, these results
183 demonstrate strong synergistic effects between auranofin and colistin against *P. aeruginosa*
184 biofilms.

185 To test whether auranofin and colistin can work together *in vivo*, we surgically inserted
186 silicone implants coated with 1-day old *P. aeruginosa* biofilms into the peritoneal cavity of
187 mice, and subsequently treated them locally with colistin (1 mg kg^{-1}), auranofin (10 μM), or a
188 combination of both drugs. Combination therapy of auranofin and colistin resulted in
189 significantly lower bacterial titer counts from the implant than either auranofin or colistin alone
190 (Fig. 6C). This confirms the synergy between auranofin and colistin in a murine model.

191 **Discussion**

192 Auranofin is approved by the FDA for the treatment of rheumatoid arthritis. It has been
193 shown to reduce inflammation of joints in rheumatic patients[44]; however, the precise
194 mechanism of how this occurs is not clear. Auranofin also exhibits anti-cancer and anti-
195 parasitic properties[39,45,46]. Furthermore, auranofin is able to kill a broad spectrum of Gram-
196 positive bacteria, and also mycobacteria[40]. All of these activities may be attributed to
197 auranofin's ability to disrupt the thiol-redox balance in cells, in part by targeting the
198 thioredoxin reductases in each of these systems[47]. Interestingly, auranofin is largely ineffective
199 against most Gram-negative bacteria, except for a few species[48-50], presumably because of lack
200 of penetration across the bacterial outer membrane[51]. Here, we have demonstrated that
201 auranofin is additionally able to inhibit virulence in *P. aeruginosa*. Despite not being able to
202 accumulate at high concentrations in cells, auranofin causes downregulation of QS, TFP
203 formation, and possibly T3SS. One possible target is Vfr, which controls all of these
204 phenotypes. Consistently, we have shown that auranofin inhibits the ability of Vfr to bind to
205 target promoter sequences in vitro. The fact that a cysteine-less Vfr variant is not inhibited in
206 vitro indicates that auranofin also targets cysteines within this protein. Interestingly, *P.*
207 *aeruginosa* does not gain resistance against auranofin even when expressing cysteine-less Vfr,
208 suggesting that it has multiple targets in cells. This is probable, given that auranofin is a general
209 thiol-targeting reagent[39]. Understanding the full mechanism of action of auranofin would
210 require identifying these unknown targets.

211 Current clinical treatment options of *P. aeruginosa* infections involve the usage of
212 carbapenems, aminoglycosides and ciprofloxacin, to name a few[16]. These drugs are often used
213 in combination or singularly in treatment. Unfortunately, many strains of *P. aeruginosa* have
214 developed resistance to such compounds and drastically reduce the pool of available treatment
215 options for clinicians[7]. Colistin remains one of the few drugs effective against most strains of

216 *P. aeruginosa*. Its usage, however, remains limited and is confined to last resort situations due
217 to its toxicity[52]. We have shown that auranofin and colistin combine synergistically to
218 completely eradicate *P. aeruginosa* biofilms, something not observed with colistin treatment
219 alone. This synergy is also observed in a murine implant model. We believe that the strong
220 synergy between auranofin and colistin works in both directions. It has been shown that
221 disrupting outer membrane permeability (here with the use of colistin) allows auranofin to
222 penetrate the cell envelope and kill Gram-negative bacteria[51], through its potential action on
223 thioredoxin reductase. At the same time, the inhibition of TFP and QS (by auranofin) during
224 biofilm development may prevent the formation of colistin-tolerant subpopulations within the
225 biofilm, thereby allowing complete eradication. The unique synergistic effects of auranofin and
226 colistin may be exploited as a new treatment regimen for *P. aeruginosa* infections. Given that
227 auranofin is already an FDA-approved drug, it may not be in the very far future that this
228 approach can be tested.
229

230 **Materials and Methods**

231 **Bacterial strains and growth conditions.** All bacterial strains used in this study are
232 summarized in Table S2. Strain PAO1 was used for all *in vivo* experiments[53]. High-throughput
233 screening of quorum sensing inhibitors was done using strain PAO1-*lasB*-*gfp*(ASV)[34]. The
234 extent of inhibition of QS was verified using strains PAO1-P_{rhlA}-*gfp*(ASV) and PAO1-P_{pqsA}-
235 *gfp*(ASV)[35]. Luria-Bertani (LB) broth (1% tryptone and 0.5% yeast extract) and agar were
236 prepared for growth of overnight cultures. M9 minimal media was prepared as previously
237 described[54]. Glass bead biofilm and flow cell biofilm experiments were conducted in ABT
238 minimal medium supplemented with 0.4 g l^{-1} glucose (ABTG)[43,55]. For plasmid maintenance
239 in *Escherichia coli*, ampicillin (Amp) was used at 200 µg ml^{-1}, tetracycline (Tc) at 12.5 µg ml^{-}
240 ^{1}. For marker selection in *P. aeruginosa*, gentamicin (Gm) was used at concentration 30 µg ml^{-}
241 ^{1}, tetracycline (Tc) at 50 µg m^{-1}, carbenicillin (Carb) at 300 µg ml^{-1}.

242

243 **Plasmid construction.** All plasmids are listed in Table S3. To construct a plasmid with desired
244 DNA fragment, gene was amplified by PCR using PAO1 genomic DNA template. Amplified
245 DNA fragment was digested with appropriate restriction enzymes (New England Biolabs) and
246 ligated into the same restriction sites of a plasmid. DH5α cells were transformed with the
247 ligation product and selected on LB plates containing appropriate antibiotics. All constructs
248 were verified by DNA sequencing (Axil Scientific, Singapore). To construct pME6031*vfr*, *vfr*,
249 together with 200 bp upstream of the ATG translational start codon was amplified and inserted
250 into the HindIII/SacI site of pME6031. To construct pUCP18vfr, *vfr* was amplified and inserted
251 into the EcoRI/HindIII site of pUCP18. To construct pME6031*vfr*Δ*5* and pUCP18*vfr*Δ*5*, the 5
252 cysteine residues in *vfr* were sequentially replaced by serine residues via site-directed
253 mutagenesis using C20S-FWD/C20S-REV, C38S-FWD/C38S-REV, C97S-FWD/C97S-REV,
254 C156S-FWD/C156S-REV and C183S-FWD/C183S-REV primer pairs. For the above,

255 pME6031*vfr* and pUCP18*vfr* were used as the templates, respectively. The resulting PCR
256 products were digested with DpnI, and transformed into DH5α and selected on LB plates
257 containing tetracycline and ampicillin, respectively.
258 To construct P_{lasR} and *rsaL* probes for EMSA, primer sequences are given in Table S4.
259
260 **QS Inhibitor Assay.** The QS inhibitor assay was conducted as previously described[34]. Briefly,
261 5-ml overnight cultures were washed in M9 minimal medium and diluted to an OD_{450} of 0.2.
262 150 µl was added into a 96-well plate that contained 150 µl of each library compound in each
263 well to appropriate concentrations. Compounds screened were from the triazine library[56] (2,920
264 compounds) (Young-Tae Chang (POSTECH)) and a ENZO commercial library of FDA-
265 approved drugs (640 compounds). The samples were incubated at 34 °C in a plate reader
266 (Victor X2, Perkin Elmer). Green fluorescence at excitation wavelength of 490 nm was
267 measured at 15 min intervals over 17 h and normalized to cell density at OD_{450}.
268
269 **Quantitative Real-time Polymerase Chain Reaction (qRT-PCR).** The qRT-PCR
270 experiment was conducted as previously described[57]. 5-ml cultures were grown (inoculated
271 with overnight cultures at 1:100 dilution) in M9 minimal medium containing appropriate
272 concentrations of auranofin/DMSO at 37 °C until OD_{450} reached ~1.0. RNeasy Protect Bacteria
273 Mini Kit with on-column DNase digestion (Qiagen) was used to extract total RNA. A Turbo
274 DNA-free vigorous protocol was used for a second round of DNase treatment (Ambion).
275 Agilent 2100 Bioanalyzer (Agilent Technologies) and Qubit 2.0 Fluorometer (Invitrogen) were
276 used to assess the integrity of the total RNA and the level of DNA contamination. Ribosomal
277 RNA contamination was removed using the Ribo-Zero Magnetic Kit (Bacteria) (Epicentre).
278 Finally, RNeasy Mini Kit (Qiagen) with on-column DNase digestion was used to extract the
279 total RNA. The purity and concentration of the RNA were determined by NanoDrop

280 spectrophotometry, and the integrity of RNA was measured using an Agilent 2200 TapeStation
281 System. The elimination of contaminating DNA was confirmed via the real-time PCR
282 amplification of the *rpoD* gene using total RNA as the template.

283 Quantitative reverse transcriptase PCR (qRT–PCR) was performed using a two-step
284 method. SuperScript III First-Strand Synthesis SuperMix kit (Cat. No. 18080-400, Invitrogen)
285 was used to synthesize first-strand cDNA from total RNA as a template. The cDNA was used
286 as a template for qRT–PCR using a SYBR Select Master Mix kit (Cat. No. 4472953, Applied
287 Biosystems by Life Technologies) on an Applied Biosystems StepOnePlus Real-Time PCR
288 System. *rpoD* was used as an endogenous housekeeping control. Melting curve analyses were
289 employed to verify the specific single-product amplification.

290

291 **Elastase Assay.** 5-ml cultures were grown (inoculated with overnight cultures at 1:100 dilution)
292 in M9 minimal medium containing appropriate concentrations of auranofin/DMSO at 37 °C
293 until OD_{450} reached ~1.0. Cells were then normalized according to OD_{450} and filtered. The
294 elastase levels within the supernatant were measured using an Elastase Assay kit (EnzChek
295 Elastase Assay kit, Life Technologies) according to manufacturer's instructions.

296

297 **Measurement of Rhamnolipid Levels.** 5-ml cultures were grown (inoculated with overnight
298 cultures at 1:100 dilution) in M9 minimal medium containing appropriate concentrations of
299 auranofin/DMSO at 37 °C until OD_{450} reached ~1.0. Cells were normalized according to OD_{450}
300 and centrifuged at 4700 x *g* for 10 min. 380 µl of acetonitrile, 100 µl of 40 mM aqueous
301 ammonium acetate and 20 µl of a 23 ppm acetonitrile solution of 16-hydroxydecanoic acid as
302 an internal standard (IS) were added to 500 µl of filtered supernatant. 10 µl was subjected to
303 LC-MS analysis.

304 The analysis of rhamnolipid (Rha-C10-C10) (Sigma-Aldrich) in culture samples was
305 performed on an Ultra High Performance Liquid Chromatography system (UFPLC Ultimates
306 3000, Dionex, CA, USA) equipped with a C18 HPLC column (100 mm x 4.5 mm, 3.5 mm, 40
307 oC, Zorbax Plus) coupled with a quadrupole-ion trap mass spectrometer (QTRAPs 5500, AB
308 Sciex, DC, USA). An acetonitrile-water gradient containing 4 mM of ammonium acetate was
309 used. Chromatography was performed with initial 40% acetonitrile for 4 min and the
310 acetonitrile concentration was raised to 90% after 20 min. The analytes were ionized in
311 negative mode using electrospray ionization and analyzed using Multiple Reaction
312 Mornitoring (MRM) on 4 mass transition pairs (Rha-C10-C10: 649.5>479.5, 649.5>169.5,
313 649.5>163; IS: 271.2>225.4). The concentration of Rha-C10-C10 in culture samples was
314 quantified using a calibration curve plotted from six Rha-C10-C10 standard solutions ranging
315 from (0 - 10ppm) spiked with a fixed concentration of 16-hydroxydecanoic acid as internal
316 standard. All the standard solutions and samples were spiked with 16-hydroxydecanoic acid as
317 an internal standard to improve accuracy of results and to remove experimental uncertainty
318 from systematic and random errors. The chromatograms were integrated using Analyst 1.5.1
319 (AB Sciex, DC, USA).
320
321 **Measurement of pyocyanin levels.** 5-ml cultures were grown (inoculated with overnight
322 cultures at 1:100 dilution) in M9 minimal medium containing appropriate concentrations of
323 auranofin/DMSO at 37 °C until OD_{450} reached ~1.0. Cells were then normalized according to
324 OD_{450} and filtered. The absorbance of the supernatant was measured at 691 nm.
325
326 **Proteomics.** 5-ml cultures were grown (inoculated with overnight cultures at 1:100 dilution)
327 in LB broth at 37 °C until OD_{450} reached ~1.0. Cells were washed, re-suspended in fresh LB
328 medium. After harvesting, the cell pellet was washed twice with 1X PBS and resuspended in

329 2 ml of lysis buffer containing 0.5 M triethylammonium bicarbonate (TEAB), 0.1 M SDS and
330 protease inhibitor cocktails (Sigma-Aldrich). The cells were ruptured by probe sonication (5
331 min of sonication, 30% amplitude) in ice slurry and the cell debris was removed by
332 centrifugation at 4 °C at 16000 x *g* for 10 min. The protein supernatant from three biological
333 replicates for each growth condition were pooled together. 200 µg of proteins from each growth
334 condition were dissolved in equal volume of Laemelli 2X sample buffer (Invitrogen, USA)
335 supplemented with 0.5% 2-mercaptoethanol. The proteins were then denatured by boiling at
336 95 °C for 5 min. 2D-SDS-PAGE was performed using 10% separating gel to concentrate the
337 protein samples, with a final 20% blocking gel which reduced protein loss by preventing the
338 proteins from leaving the gel.

339 Gel fragments were submitted for iTRAQ proteomics analysis. Briefly, fragments were
340 reduced with 5 mM tris 2-carboxyethyl phosphine hydrochloride (TCEP) followed by
341 alkylation with 10 mM methyl methanethiosulfonate (MMTS). They were subsequently
342 dehydrated with 100% acetonitrile (ACN) and digested using sequencing grade modified
343 trypsin (Promega, USA) at 37 °C for 20 h. Peptides were dried using 50% ACN/5% acetic acid
344 mixture and dried under vacuum.

345 iTRAQ labeling of peptide samples was performed using the iTRAQ reagent multiplex
346 kit (Applied Biosystems, Life Technologies) according to manufacturer's instructions. Both
347 labelled samples were pooled and reconstituted in Buffer A (10 mM KH2PO4, 25% acetonitrile,
348 pH 2.85), and fractionated using PolySULFOETHYL A SCX column by HPLC (Shimadzu,
349 Japan) at a flow rate of 1.0 ml min^{-1}. The collected fractions were desalted with Sep-Pak Vac
350 C-18 cartridges (Waters, USA), dried under vacuum and reconstituted in 0.1% formic acid for
351 LC-MS/MS analysis. LC-MS/MS analysis was conducted using a Q-Star Elite mass
352 spectrometer (Applied Biosystems, USA) coupled to a micro flow HPLC system (Shimadzu,
353 Japan).

354 **Immunoblot analysis.** 5-ml cultures were grown (inoculated with overnight cultures at 1:100
355 dilution) in LB broth at 37 °C until OD_{450} reached ~1.0. Cells were normalized according to
356 OD_{450} and mixed with equal amounts of 2X Laemmli reducing buffer and subjected to SDS-
357 page on 2 separate gels. Protein bands for both of the gels were transferred to polyvinylidene
358 fluoride (PVDF) membranes (Immun-Blot® 0.2 µm, Bio-Rad) using semi-dry electroblotting
359 system (Trans-Blot® TurboTM Transfer System, Bio-Rad). Membranes were blocked by 1X
360 casein blocking buffer (Sigma). α-Vfr was provided by Katrina Forest (University of
361 Wisconsin-Madison) and used at a dilution of 1:25,000. α-rabbit IgG secondary antibody
362 conjugated to HRP (from donkey) was purchased from GE Healthcare and used at 1:5,000
363 dilution. Luminata Forte Western HRP Substrate (Merck Milipore) was used to develop the
364 membranes and protein bands were visualized by G:BOX Chemi XT 4 (Genesys version
365 1.3.4.0, Syngene).
366
367 **Motility assay.** 10-ml overnight cultures were grown in LB broth at 37 °C and normalized to
368 the lowest cell density according to OD_{450}. To determine swimming motility, 0.3% LB agar
369 containing appropriate concentrations of auranofin/DMSO was point inoculated with the
370 overnight into the middle and incubated at 30 °C for 24 h. To determine swarming motility,
371 0.5% LB agar containing appropriate concentrations of auranofin/DMSO was point inoculated
372 with the overnight culture at the surface and incubated at 37 °C for 24 h. To determine twitching
373 motility, 1% LB agar containing appropriate concentrations of auranofin/DMSO was point
374 inoculated at the agar-plate interface with an overnight colony of plated cells and incubated at
375 37 °C for 48 h. The agar was subsequently removed and adhered cells were stained with 0.05%
376 Coomassie blue G250 (Sigma) (40% methanol, 10% acetic). Plate images were visualized by
377 G-BOX Chemi XT 4 (Genesys version 1.3.4.0, Syngene).
378

379 **Purification of Vfr and its variant.** Purification of Vfr and VfrΔ5 was performed according
380 to a procedure described previously with some modifications[58]. Vfr and VfrΔ5 were purified
381 from pUCP-*vfr* and pUCP-*vfr*Δ*5*, respectively. For each strain, a 500-ml culture (inoculated
382 from a mid-log culture at 1:100 dilution) was grown overnight in LB broth at 37 °C. Cells for
383 each strain were harvested by centrifugation at 4,700 x *g* for 20 min. Cells were resuspended
384 in 20 ml of 20 mM Tris.HCl, pH 8.0 containing 1 mM phenylmethylsulfonyl fluoride (PMSF),
385 100 μg ml^{-1} lysozyme and 50 μg ml^{-1} DNase I. The resuspended cells were lysed by a single
386 passage through a high pressure French Press (French Press G-M, Glen Mills) homogenizer at
387 20,000 psi. Unbroken cells were removed by centrifugation at 5,000 x *g* for 10 min. The cell
388 lysate was collected and centrifuged at 100,000 x *g* for 1 h in an ultracentrifuge (Model XL-
389 90, Beckman Coulter). The supernatant was collected, loaded into a column packed with 1 ml
390 of cyclic adenosine monophosphate (cAMP) agarose column (Sigma Aldrich), which had been
391 pre-equilibrated with 10 ml of buffer A (25 mM Tris.HCl/150 mM NaCl, pH 8.0) and incubated
392 at 4 °C for 1 h, by rocking. The resin mixture was later allowed to drain by gravity. The filtrate
393 was collected, reloaded into column and drained as above. The column was washed with 4 x
394 10 ml buffer A and then eluted with 4 x 4 ml of buffer B (25 mM Tris.HCl/150 mM NaCl, pH
395 8.0) each with increasing amounts of free cAMP to 0.5, 5, 10 and 25 mM. The eluted fractions
396 were concentrated in a 10 kDa cut-off ultra-filtration device (Amicon Ultra, Merck Millipore)
397 by centrifugation at 4,000 x *g* to ~200 μl. The concentrated sample was mixed with equal
398 amounts of 2X Laemmli reducing buffer and subjected to SDS-PAGE analyses and
399 immunoblotting. Fractions containing pure Vfr and VfrΔ5 were collected and used.
400
401 **Electromobility Shift Assay (EMSA).** 0.5 μl of 4 mM auranofin was serial diluted in 10 μl of
402 1X Buffer C (20 mM Tris.HCl/200 mM KCl/2mM EDTA/1% glycerol/0.1 mg BSA, pH 8.0)
403 and incubated with 4.8 μl of purified protein at appropriate concentration at room temperature

404 for 10 min. The mixture was then combined with buffer D (1X Buffer C/500 μM cAMP/432
405 nM DNA probe/432 nM rsaL) and incubated for 20 min. 5 μl of 5X DNA loading dye
406 (COMPOSITION) was added and the reaction was subjected to PAGE analyses on a 6% TBE
407 gel (Tris.HCl/Boric acid/EDTA, pH8.0). DNA bands were stained by immersing the gel in 3X
408 GelRed staining solution (3,000X GelRed stain/100mM NaCl) (Biotium) for 30 min followed
409 by visualization by G-BOX Chemi XT 4 (Genesys version 1.3.4.0, Syngene)
410

411 **Glass beads biofilm assay.** The glass bead biofilm assays were performed as described by
412 Konrat, K. *et al*[59]. *Pseudomonas aeruginosa* PAO1 was cultured overnight in 2 ml LB broth at
413 37°C shaking condition (200 rpm). The overnight culture was centrifuged at 13,000 x *g* for 2
414 min and the supernatant was discarded. The cell pellet was washed once with 2 ml of 0.9%
415 NaCl, followed by centrifugation to pellet the cells. After the wash, cells were then resuspended
416 and adjusted to OD_{600} of 0.1 with ABTG before 1 ml of the culture was pipetted into each well
417 of the 24-well, flat-bottom plate (Nunclon® Δ Multidishes, ThermoFisher Scientific). One
418 sterile 5-mm glass bead (Merck KGaA, Darmstadt, Germany) was placed into each well prior
419 to incubation in 37 °C shaking condition (100 rpm) for 24 h for biofilm formation.

420 After 24 h of cultivation, the biofilm-coated glass beads were gently picked and
421 submerged in 0.9% NaCl solution for 3 times using sterile tweezer to remove the unbound cells
422 before transferring to new 24-well plates that consist of different concentrations of colistin
423 sulfate (Sigma-Aldrich) and auranofin (Sigma-Aldrich) combinations. After 24 h of treatment
424 in 37 °C shaking condition (100 rpm), each glass bead was then transferred to an 1.5-ml
425 Eppendorf tube containing 1 ml of 0.9% NaCl before subjected to water-bath sonication using
426 Elmasonic P120H (Elma, Germany; power=80% and frequency=37 KHz) for 10 min and
427 rigorous vortex for 5 min to disrupt the biofilms. For enumeration of viable cells per glass bead,
428 the samples were serially diluted, plated on LB agar followed by incubation overnight at 37 °C

429 for colony forming unit (c.f.u.) count. Biological triplicates were performed and the average
430 c.f.u. count per glass bead in each condition was determined.
431
432 **Dynamic development of *P. aeruginosa* biofilm in flow cell.** The assembly of flow chamber
433 and experimental setup has been described previously[43,57,60]. Bacterial strains were cultured
434 overnight in 2 ml of LB medium in 37 °C shaking incubator (200 rpm). For marker selection
435 in *P. aeruginosa*, 30 μg ml^{-1} gentamicin or 50 μg ml^{-1} tetracycline was used. The overnight
436 cultures were adjusted to OD_{600} of 0.1 with ABTG and 500 μl of the diluted cultured was
437 injected into each flow chamber and was incubated for 1 h without medium flow. Wild-type
438 PAO1 were fed with ABTG containing either freshly prepared 2 μM auranofin or DMSO (as
439 solvent control) at the rate of 4 ml h^{-1} via peristaltic pump (Cole-Parmer®) in 37 ºC condition.
440 QS-null strain PAO1 Δ*lasI*Δ*rhlI* was used as control. At time-point 6 h, 24 h, 48 h and 72 h, 1
441 flow cell from each condition was removed from the system and the bacterial cells were stained
442 with 300 μl of 3.34 μM SYTO9 and 20 μM propidium iodide (PI) (LIVE/DEAD™ *Bac*Light™
443 Bacterial Viability Kit, Molecular Probes) for 15 min for the observation of live and dead cells
444 respectively using confocal laser scanning microscopy. The experiments were performed in
445 triplicate and representative images are shown.
446
447 **Auranofin and colistin treatment on *P. aeruginosa* flow cell biofilm.** The flow cell biofilm
448 experiments were setup as mentioned above. The GFP-tagged *P. aeruginosa* was cultured for
449 48 h prior to treatment with; DMSO (solvent control), or 1 μM auranofin single treatment, or
450 10 μg ml^{-1} colistin single treatment, or 1 μM auranofin and 10 μg ml^{-1} colistin combination
451 treatment for 24 h. Then, the dead cells were stained with PI as described above prior to
452 confocal microscopy imaging. The experiments were performed in triplicate and
453 representative images are shown.

454 **Confocal microscopy imaging.** The microscopy images of the biofilms were captured and
455 acquired using LSM 780 confocal laser scanning microscopy (Carl Zeiss, Germany). Either
456 20x/0.80 DICII or 40x/1.30 DICIII (oil) objective lens was used for confocal imaging. 488 nm
457 argon multiline laser and HeNe 561 nm laser were used to monitor the GFP-expressing or
458 SYTO9-stained live cells and PI-stained dead cells respectively. The acquired images were
459 further processed using IMARIS version 9 (Bitplane AG, Zurich, Switzerland).
460
461 **Image analysis (for biofilm development in flow cells).** The confocal images were processed
462 using COMSTAT2 program to quantify the three-dimensional biofilm image stack as
463 previously described[61-63]. The biofilm structures were described with 3 variables (biofilm
464 biomass, mean thickness and roughness coefficient). All COMSTAT2 parameters are fixed at
465 default setting prior to image analysis.
466
467 **Mouse implant infection model.** All animal experiments were carried out in accordance to
468 the NACLAR Guidelines and Animal and Birds (Care and Use of Animals for Scientific
469 Purposes) Rules by Agri-Food & Authority of Singapore (AVA), with authorization and
470 approval by the Institutional Care and Use Committee (IACUC) and Nanyang Technological
471 University, under the permit number A-0191 AZ.
472 Seven to eight week-old female BALB/c mice (Taconic M&B A/S) were used in this
473 experiment. The mouse implant infection model experimental setup was carried out as
474 described previously[64,65]. *Pseudomonas aeruginosa* was cultured overnight in 2 ml of LB
475 medium in 37 °C shaking incubator (200 rpm). The overnight culture was centrifuged at 13,000
476 x *g* for 1 min and the supernatant was discarded prior to washing with 0.9% NaCl at equal
477 volume. The cell pellet was resuspended and diluted to OD_{600} of 0.1 with 0.9% NaCl. The
478 biofilms were developed on cylindrical implants (4 mm × 5 mm Ø) in the diluted culture for

479 20 h at 37 °C with shaking condition (110 rpm). The implants were then washed 3 times
480 with 0.9% NaCl to remove the unbound cells, before insertion into the peritoneal cavity of
481 the mouse that was anesthetized with 100 mg kg^{-1} ketamine and 10 mg kg^{-1} xylene. 24 h
482 after the insertion, 200 µl of the treatment; control (DMSO), or 10 µM auranofin, or 1 mg
483 kg^{-1} colistin; or 10 µM auranofin and 1 mg kg^{-1} colistin was injected into the peritoneal
484 cavity and the second treatment was given at 30 hours-post-infection. The mice were
485 sacrificed at 48 hours-post-infection and the implants were retrieved, sonicated in a water-
486 bath Elmasonic P120H (Elma, Germany; power=80% and frequency=37 KHz) for 10 min and
487 vortexed rigorously 3 times of 10 seconds each, before subjected to c.f.u plating on LB agar
488 plates to determine the viable bacterial cells on the implants. Experiments were performed
489 with 10 replicates, and the results are shown as the mean. Implants from the mice that died
490 before the experiment endpoint were not included in the statistical analysis.

491 **Acknowledgements**

492 We thank Young-Tae Chang (POSTECH) for allowing access to small molecule libraries used
493 in this study. We acknowledge Song Lin Chua (SCELSE) for his help in processing and
494 submitting our samples for proteomics analysis. We thank Yingying Li (SCELSE) for her
495 guidance in RT-PCR experiments. We are grateful to Katrina Forest (University of Wisconsin-
496 Madison) for the generous gift of the α−Vfr antibody. This research was supported by the
497 National Research Foundation and the Ministry of Education of Singapore under its Research
498 Centre of Excellence Programme. M.G., S.-S.C., L.Y., L.Z.W.T., and Z.H. have filed an
499 international patent application (PCT/SG2016/050436, filed 6th September 2016) and granted
500 a US patent (US 10,258,640 B2, dated 16th April 2019) on the work described in this
501 manuscript.

502

503 **Author Contributions**

504 L.Y., M.G., and S.-S.C. conceived the project and directed the study. Z.H. conducted the QS
505 inhibitor screening assay. L.Z.W.T. conducted all biochemical experiments. J.K.H.Y. and
506 M.M.S.S. performed the mouse model and the biofilm experiments. B.Y.W. conducted the
507 rhamnolipid analysis with supervision from S.F.Y.L.. L.Z.W.T., J.K.H.Y, and S.-S.C. wrote
508 the manuscript with input from all authors.

509 **References**

510 1 Vincent, J.-L. *et al.* The prevalence of nosocomial infection in intensive care units in
511 Europe: results of the European Prevalence of Infection in Intensive Care (EPIC) Study.
512 *Jama* **274**, 639-644 (1995).

513 2 Palmer, K. L., Mashburn, L. M., Singh, P. K. & Whiteley, M. Cystic fibrosis sputum
514 supports growth and cues key aspects of Pseudomonas aeruginosa physiology. *Journal*
515 *of bacteriology* **187**, 5267-5277 (2005).

516 3 Church, D., Elsayed, S., Reid, O., Winston, B. & Lindsay, R. Burn wound infections.
517 *Clinical microbiology reviews* **19**, 403-434 (2006).

518 4 Ringen, L. M. & Drake, C. H. A study of the incidence of Pseudomonas aeruginosa
519 from various natural sources. *Journal of bacteriology* **64**, 841 (1952).

520 5 Cole, S. J., Records, A. R., Orr, M. W., Linden, S. B. & Lee, V. T. Catheter-associated
521 urinary tract infection by Pseudomonas aeruginosa is mediated by exopolysaccharide-
522 independent biofilms. *Infection and immunity* **82**, 2048-2058 (2014).

523 6 Mittal, R., Aggarwal, S., Sharma, S., Chhibber, S. & Harjai, K. Urinary tract infections
524 caused by Pseudomonas aeruginosa: a minireview. *Journal of infection and public*
525 *health* **2**, 101-111 (2009).

526 7 Hirsch, E. B. & Tam, V. H. Impact of multidrug-resistant Pseudomonas aeruginosa
527 infection on patient outcomes. *Expert review of pharmacoeconomics & outcomes*
528 *research* **10**, 441-451 (2010).

529 8 Nathwani, D., Raman, G., Sulham, K., Gavaghan, M. & Menon, V. Clinical and
530 economic consequences of hospital-acquired resistant and multidrug-resistant
531 Pseudomonas aeruginosa infections: a systematic review and meta-analysis.
532 *Antimicrobial resistance and infection control* **3**, 32 (2014).

533 9 Nikaido, H. Molecular basis of bacterial outer membrane permeability revisited.
534 *Microbiol. Mol. Biol. Rev.* **67**, 593-656 (2003).
535 10 Li, X.-Z., Livermore, D. M. & Nikaido, H. Role of efflux pump (s) in intrinsic
536 resistance of Pseudomonas aeruginosa: resistance to tetracycline, chloramphenicol, and
537 norfloxacin. *Antimicrobial agents and chemotherapy* **38**, 1732-1741 (1994).
538 11 Poole, K., Krebes, K., McNally, C. & Neshat, S. Multiple antibiotic resistance in
539 Pseudomonas aeruginosa: evidence for involvement of an efflux operon. *Journal of*
540 *bacteriology* **175**, 7363-7372 (1993).
541 12 Sanders, C. C. & Sanders Jr, W. E. β-Lactam resistance in gram-negative bacteria:
542 global trends and clinical impact. *Clinical Infectious Diseases* **15**, 824-839 (1992).
543 13 Okamoto, K., Gotoh, N. & Nishino, T. Pseudomonas aeruginosa reveals high intrinsic
544 resistance to penem antibiotics: penem resistance mechanisms and their interplay.
545 *Antimicrobial agents and chemotherapy* **45**, 1964-1971 (2001).
546 14 Costerton, J. W., Stewart, P. S. & Greenberg, E. P. Bacterial biofilms: a common cause
547 of persistent infections. *Science* **284**, 1318-1322 (1999).
548 15 Høiby, N., Bjarnsholt, T., Givskov, M., Molin, S. & Ciofu, O. Antibiotic resistance of
549 bacterial biofilms. *International journal of antimicrobial agents* **35**, 322-332 (2010).
550 16 Driscoll, J. A., Brody, S. L. & Kollef, M. H. The epidemiology, pathogenesis and
551 treatment of Pseudomonas aeruginosa infections. *Drugs* **67**, 351-368 (2007).
552 17 Chiang, W.-C. *et al.* Extracellular DNA shields against aminoglycosides in
553 Pseudomonas aeruginosa biofilms. *Antimicrobial agents and chemotherapy* **57**, 2352-
554 2361 (2013).
555 18 Fong, J. *et al.* Disulfide bond-containing ajoene analogues as novel quorum sensing
556 inhibitors of Pseudomonas aeruginosa. *Journal of medicinal chemistry* **60**, 215-227
557 (2017).

558 19 Fong, J. *et al.* Combination therapy strategy of quorum quenching enzyme and quorum
559 sensing inhibitor in suppressing multiple quorum sensing pathways of P. aeruginosa.
560 *Scientific reports* **8**, 1-11 (2018).
561 20 Alhede, M. *et al.* Pseudomonas aeruginosa recognizes and responds aggressively to the
562 presence of polymorphonuclear leukocytes. *Microbiology* **155**, 3500-3508 (2009).
563 21 Hentzer, M. *et al.* Attenuation of Pseudomonas aeruginosa virulence by quorum sensing
564 inhibitors. *The EMBO journal* **22**, 3803-3815 (2003).
565 22 Suh, S.-J. *et al.* Effect of vfr mutation on global gene expression and catabolite
566 repression control of Pseudomonas aeruginosa. *Microbiology* **148**, 1561-1569 (2002).
567 23 Wolfgang, M. C., Lee, V. T., Gilmore, M. E. & Lory, S. Coordinate regulation of
568 bacterial virulence genes by a novel adenylate cyclase-dependent signaling pathway.
569 *Developmental cell* **4**, 253-263 (2003).
570 24 Coggan, K. A. & Wolfgang, M. C. Global regulatory pathways and cross-talk control
571 Pseudomonas aeruginosa environmental lifestyle and virulence phenotype. *Current*
572 *issues in molecular biology* **14**, 47 (2012).
573 25 Davinic, M., Carty, N. L., Colmer-Hamood, J. A., San Francisco, M. & Hamood, A. N.
574 Role of Vfr in regulating exotoxin A production by Pseudomonas aeruginosa.
575 *Microbiology* **155**, 2265 (2009).
576 26 Beatson, S. A., Whitchurch, C. B., Sargent, J. L., Levesque, R. C. & Mattick, J. S.
577 Differential regulation of twitching motility and elastase production by Vfr in
578 Pseudomonas aeruginosa. *Journal of bacteriology* **184**, 3605-3613 (2002).
579 27 Deng, W. *et al.* Assembly, structure, function and regulation of type III secretion
580 systems. *Nature Reviews Microbiology* **15**, 323 (2017).
581 28 Mattick, J. S. Type IV pili and twitching motility. *Annual Reviews in Microbiology* **56**,
582 289-314 (2002).

583 29 Albus, A. M., Pesci, E. C., Runyen-Janecky, L. J., West, S. & Iglewski, B. H. Vfr
584 controls quorum sensing in Pseudomonas aeruginosa. *Journal of Bacteriology* **179**,
585 3928-3935 (1997).
586 30 Rutherford, S. T. & Bassler, B. L. Bacterial quorum sensing: its role in virulence and
587 possibilities for its control. *Cold Spring Harbor Perspectives in Medicine* **2**, a012427
588 (2012).
589 31 McShan, A. C. & De Guzman, R. N. The bacterial type III secretion system as a target
590 for developing new antibiotics. *Chemical biology & drug design* **85**, 30-42 (2015).
591 32 Jakobsen, T. H. *et al.* Food as a source for quorum sensing inhibitors: iberin from
592 horseradish revealed as a quorum sensing inhibitor of Pseudomonas aeruginosa. *Appl.*
593 *Environ. Microbiol.* **78**, 2410-2421 (2012).
594 33 Duncan, M. C., Linington, R. G. & Auerbuch, V. Chemical inhibitors of the type three
595 secretion system: disarming bacterial pathogens. *Antimicrobial agents and*
596 *chemotherapy* **56**, 5433-5441 (2012).
597 34 Hentzer, M. *et al.* Inhibition of quorum sensing in Pseudomonas aeruginosa biofilm
598 bacteria by a halogenated furanone compound. *Microbiology* **148**, 87-102 (2002).
599 35 Yang, L. *et al.* Computer-aided identification of recognized drugs as Pseudomonas
600 aeruginosa quorum-sensing inhibitors. *Antimicrobial agents and chemotherapy* **53**,
601 2432-2443 (2009).
602 36 Anyan, M. E. *et al.* Type IV pili interactions promote intercellular association and
603 moderate swarming of Pseudomonas aeruginosa. *Proceedings of the National Academy*
604 *of Sciences* **111**, 18013-18018 (2014).
605 37 Burrows, L. L. Pseudomonas aeruginosa twitching motility: type IV pili in action.
606 *Annual review of microbiology* **66**, 493-520 (2012).

607 38 Fuchs, E. L. *et al.* The Pseudomonas aeruginosa Vfr regulator controls global virulence
608 factor expression through cyclic AMP-dependent and-independent mechanisms.
609 *Journal of bacteriology* **192**, 3553-3564 (2010).
610 39 Di Sarra, F., Fresch, B., Bini, R., Saielli, G. & Bagno, A. Reactivity of auranofin with
611 selenols and thiols–implications for the anticancer activity of gold (I) compounds.
612 *European Journal of Inorganic Chemistry* **2013**, 2718-2727 (2013).
613 40 Harbut, M. B. *et al.* Auranofin exerts broad-spectrum bactericidal activities by targeting
614 thiol-redox homeostasis. *Proceedings of the National Academy of Sciences* **112**, 4453-
615 4458 (2015).
616 41 Rodesney, C. A. *et al.* Mechanosensing of shear by Pseudomonas aeruginosa leads to
617 increased levels of the cyclic-di-GMP signal initiating biofilm development.
618 *Proceedings of the National Academy of Sciences* **114**, 5906-5911 (2017).
619 42 Solano, C., Echeverz, M. & Lasa, I. Biofilm dispersion and quorum sensing. *Current*
620 *opinion in microbiology* **18**, 96-104 (2014).
621 43 Chua, S. L. *et al.* Selective labelling and eradication of antibiotic-tolerant bacterial
622 populations in Pseudomonas aeruginosa biofilms. *Nature communications* **7**, 1-11
623 (2016).
624 44 Finkelstein, A. *et al.* Auranofin. New oral gold compound for treatment of rheumatoid
625 arthritis. *Annals of the rheumatic diseases* **35**, 251-257 (1976).
626 45 Debnath, A. *et al.* A high-throughput drug screen for Entamoeba histolytica identifies
627 a new lead and target. *Nature medicine* **18**, 956 (2012).
628 46 Park, S.-H., Lee, J. H., Berek, J. S. & Hu, M. C.-T. Auranofin displays anticancer
629 activity against ovarian cancer cells through FOXO3 activation independent of p53.
630 *International journal of oncology* **45**, 1691-1698 (2014).

631 47 Becker, K., Gromer, S., Schirmer, R. H. & Müller, S. Thioredoxin reductase as a
632 pathophysiological factor and drug target. *European journal of biochemistry* **267**, 6118-
633 6125 (2000).
634 48 Elkashif, A. & Seleem, M. N. Investigation of auranofin and gold-containing analogues
635 antibacterial activity against multidrug-resistant Neisseria gonorrhoeae. *Scientific*
636 *reports* **10**, 1-9 (2020).
637 49 Jang, H.-I. & Eom, Y.-B. Antibiofilm and antibacterial activities of repurposing
638 auranofin against Bacteroides fragilis. *Archives of microbiology*, 1-10 (2019).
639 50 Epstein, T. D., Wu, B., Moulton, K. D., Yan, M. & Dube, D. H. Sugar-modified analogs
640 of auranofin are potent inhibitors of the gastric pathogen Helicobacter pylori. *ACS*
641 *infectious diseases* **5**, 1682-1687 (2019).
642 51 Thangamani, S. *et al.* Antibacterial activity and mechanism of action of auranofin
643 against multi-drug resistant bacterial pathogens. *Scientific reports* **6**, 1-13 (2016).
644 52 Javan, A. O., Shokouhi, S. & Sahraei, Z. A review on colistin nephrotoxicity. *European*
645 *journal of clinical pharmacology* **71**, 801-810 (2015).
646 53 Holloway, B. & Morgan, A. Genome organization in Pseudomonas. *Annual Reviews in*
647 *Microbiology* **40**, 79-105 (1986).
648 54 Miller, J. (Cold Spring Harbor Laboratory, Cold Spring Harbor, NY, 1972).
649 55 Chua, S. L. *et al.* Bis-(3′-5′)-cyclic dimeric GMP regulates antimicrobial peptide
650 resistance in Pseudomonas aeruginosa. *Antimicrobial agents and chemotherapy* **57**,
651 2066-2075 (2013).
652 56 Moon, H.-S. *et al.* A novel microtubule destabilizing entity from orthogonal synthesis
653 of triazine library and zebrafish embryo screening. *Journal of the American Chemical*
654 *Society* **124**, 11608-11609 (2002).

655 57 Chua, S. L. *et al.* Dispersed cells represent a distinct stage in the transition from
656 bacterial biofilm to planktonic lifestyles. *Nature communications* **5**, 1-12 (2014).
657 58 Fuchs, E. L. *et al.* In vitro and in vivo characterization of the Pseudomonas aeruginosa
658 cyclic AMP (cAMP) phosphodiesterase CpdA, required for cAMP homeostasis and
659 virulence factor regulation. *Journal of bacteriology* **192**, 2779-2790 (2010).
660 59 Konrat, K. *et al.* The bead assay for biofilms: a quick, easy and robust method for
661 testing disinfectants. *PloS one* **11**, e0157663 (2016).
662 60 Sternberg, C. & Tolker-Nielsen, T. Growing and analyzing biofilms in flow cells.
663 *Current protocols in microbiology*, 1B. 2.1-1B. 2.15 (2006).
664 61 Heydorn, A. *et al.* Quantification of biofilm structures by the novel computer program
665 COMSTAT. *Microbiology* **146 (Pt 10)**, 2395-2407, doi:10.1099/00221287-146-10-
666 2395 (2000).
667 62 Vorregaard, M. *Comstat2-a modern 3D image analysis environment for biofilms*,
668 Citeseer, (2008).
669 63 Chew, S. C. *et al.* Matrix polysaccharides and SiaD diguanylate cyclase alter
670 community structure and competitiveness of Pseudomonas aeruginosa during dual-
671 species biofilm development with Staphylococcus aureus. *MBio* **9**, e00585-00518
672 (2018).
673 64 Christensen, L. D. *et al.* Impact of Pseudomonas aeruginosa quorum sensing on biofilm
674 persistence in an in vivo intraperitoneal foreign-body infection model. *Microbiology*
675 **153**, 2312-2320 (2007).
676 65 Chua, S. L. *et al.* In vitro and in vivo generation and characterization of Pseudomonas
677 aeruginosa biofilm-dispersed cells via c-di-GMP manipulation. *Nature protocols* **10**,
678 1165-1180 (2015).

679

680 **Figures**

681 **Figure 1**

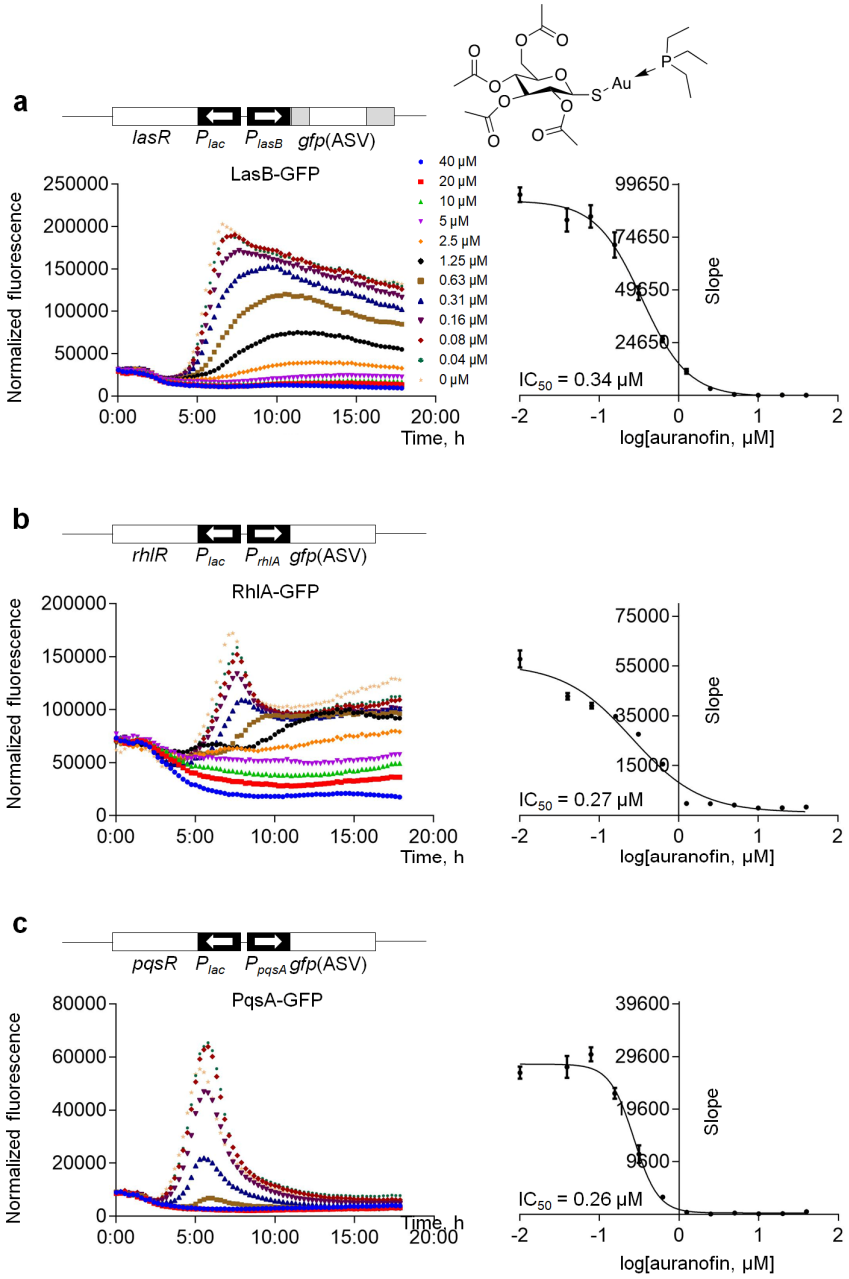

682

683 **Figure 1.** Auranofin inhibits all levels of QS with minimal effects on cell growth.
684 Representative fluorescence induction profiles (relative fluorescence units normalized to cell
685 density, over time) for (a) LasR-mediated expression of LasB-GFP, (b) RhlR-mediated
686 expression of P_{rhlA}-*gfp*, and (c) PqsR-mediated expression of P_{pqsA}-*gfp*, in the presence of

687 indicated concentrations of auranofin, whose chemical structure is shown on the top. Dose-
688 dependent inhibition curves for each assay are plotted on the right. Error bars represent
689 standard deviation from technical triplicates.

690 **Figure 2**

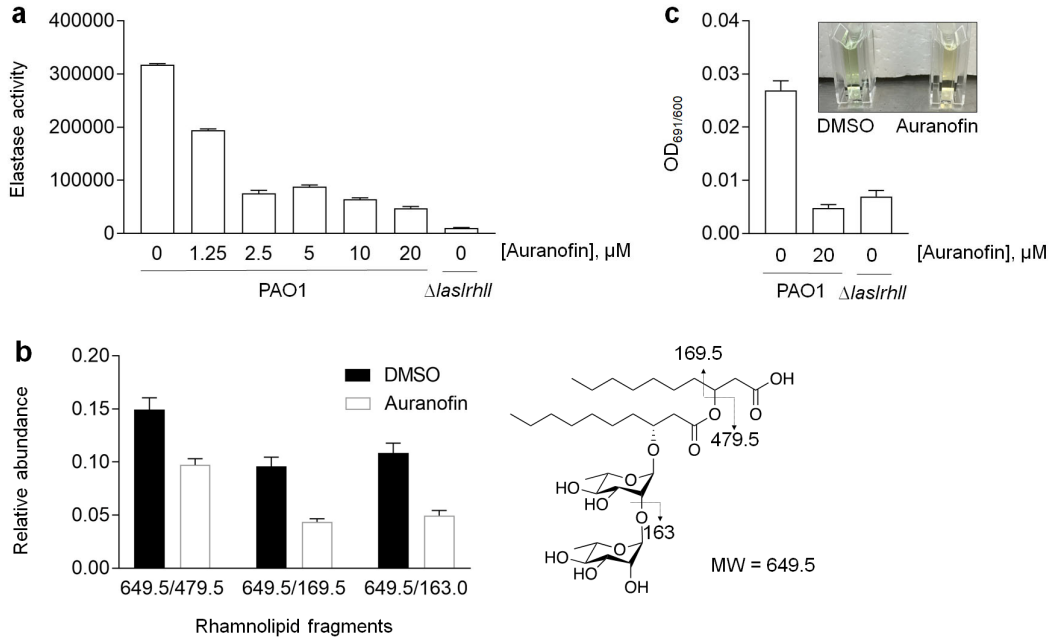

691

692 **Figure 2.** The production of key QS-controlled virulence factors is reduced in the presence of
693 auranofin. (a) Elastase activity in the supernatants of PAO1 and Δ*lasIrhlI* cultures treated with
694 indicated concentrations of auranofin. (b) Relative abundance of rhamnolipid fragments
695 isolated from PAO1 cells treated with 20 μM auranofin, as quantified using multiple reaction
696 monitoring mass spectrometry. The chemical structure of rhamnolipid and its measured
697 fragments are shown on the right. (c) Relative levels of pyocyanin in supernatants of PAO1
698 and Δ*lasIrhlI* cultures treated with indicated concentrations of auranofin, as measured at
699 absorbance at 691 nm. Error bars represent standard deviation from biological triplicates.

700 **Figure 3**

701 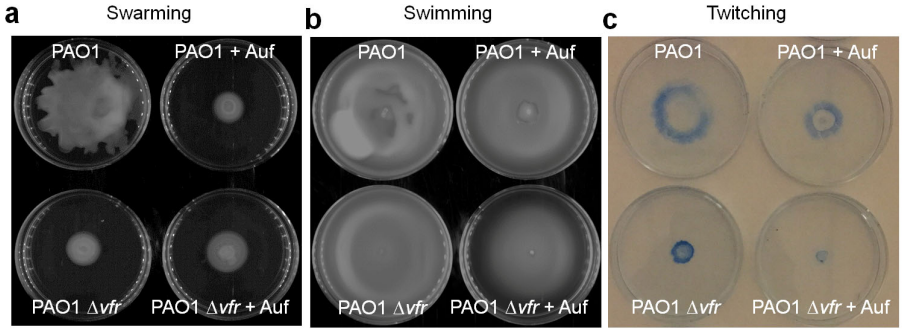

702 **Figure 3.** Motility phenotypes that depend on TFP (i.e. swarming and twitching) are reduced
703 in the presence of auranofin. (a) Swarming (0.5% LB agar), (b) swimming (0.3% LB agar),
704 and (c) twitching (1% LB agar) motilities of PAO1 and PAO1 Δ*vfr* strains in the presence or
705 absence of 20 μM auranofin. For twitching, cells at the base of the plates were stained with
706 Coomassie blue.

707 **Figure 4**

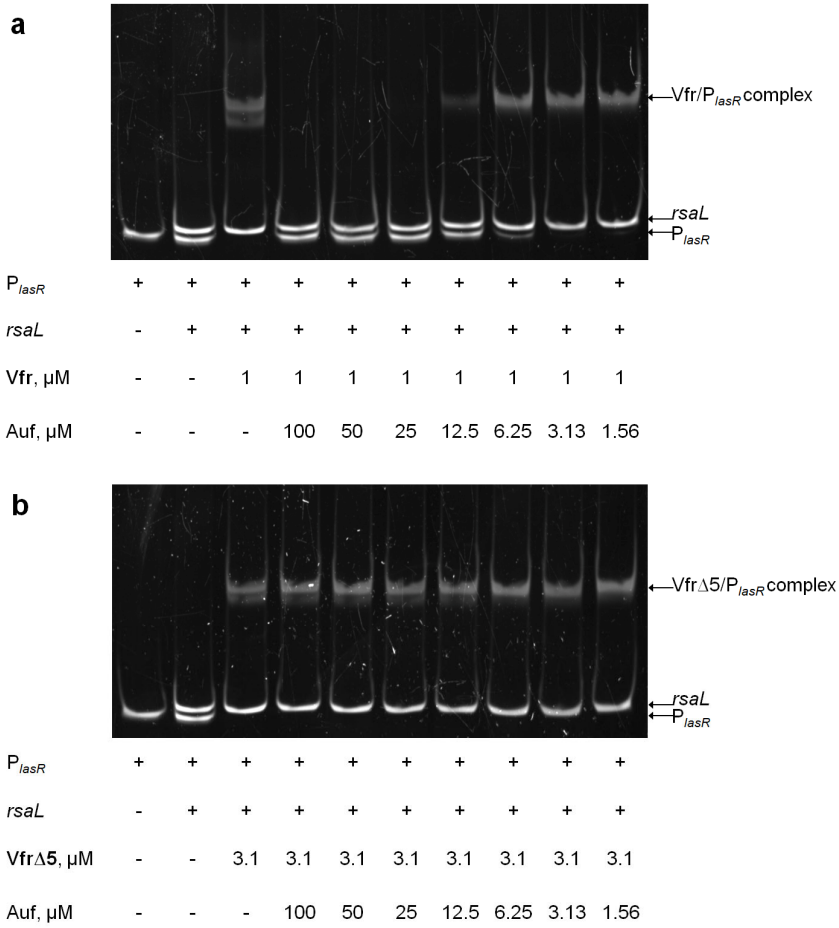

708

709 **Figure 4.** Auranofin inhibits Vfr binding to target promoter sequences *in vitro* by reacting with
710 cysteine residues. Representative polyacrylamide gels showing specific binding of (a) Vfr and
711 (b) VfrΔ5 to P_{lasR}, in the presence of indicated concentrations of auranofin. Vfr and VfrΔ5 bind
712 specifically to the target promoter sequence at ~1 and 3 μM, respectively (see Fig. S3). The
713 coding region of the gene *rsaL* is used as a probe to control for non-specific binding.

714 **Figure 5**

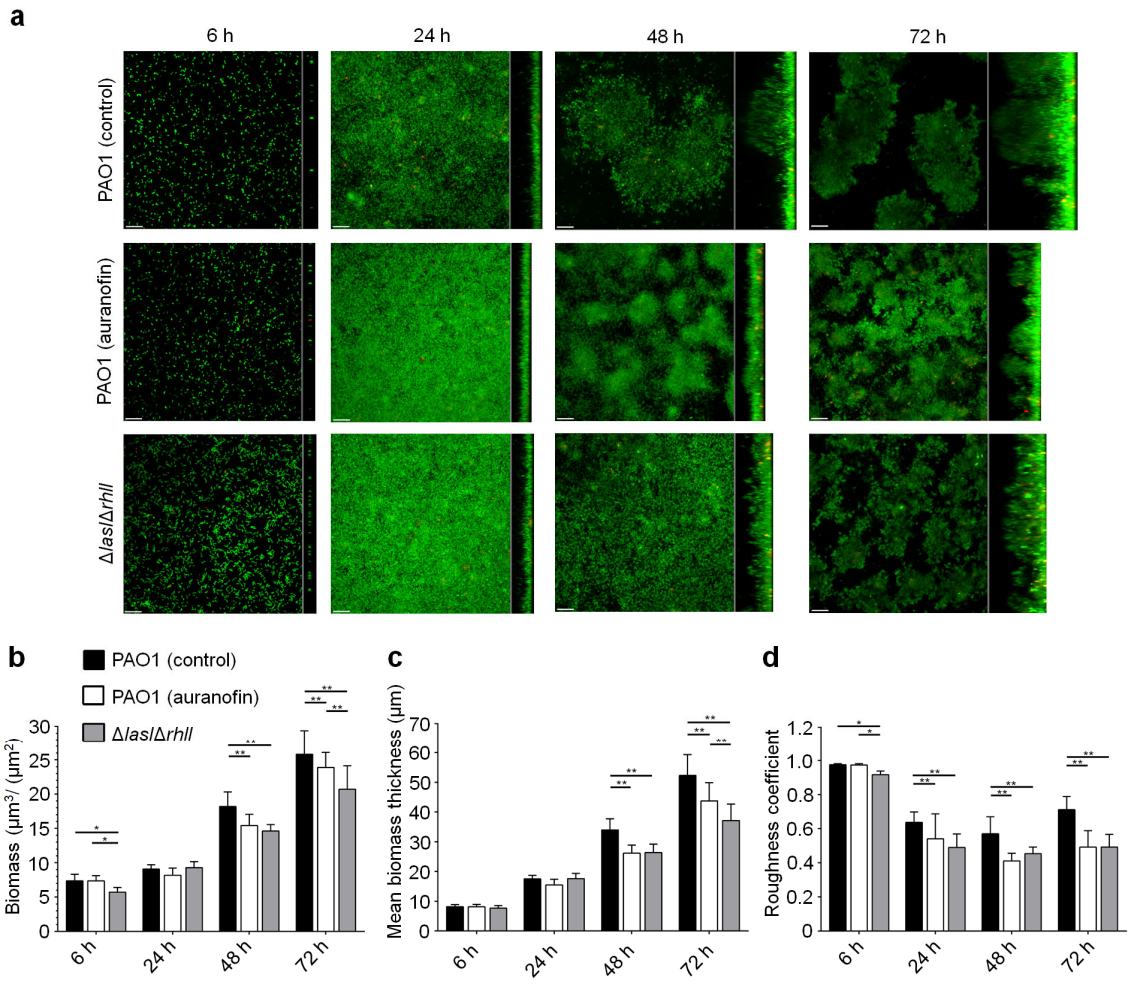

715

716 **Figure 5.** Auranofin attenuates the formation of mushroom-shaped structures in *Pseudomonas*
717 *aeruginosa* biofilms. (a) Confocal fluorescence microscopy images illustrating the
718 development of wild-type *P. aeruginosa* PAO1 biofilms in the presence or absence of auranofin
719 over 72 h in flow chambers. QS-defective mutant strain PAO1 Δ*lasI*Δ*rhlI* was used as control.
720 Biofilms were stained with SYTO9 before imaging. Biological replicates were performed, and
721 a representative image for each condition/time point is shown. Scale bar, 20 μm. Biofilm
722 parameters including (b) biomass, (c) mean biomass thickness, and (d) roughness coefficient,
723 were quantified via analyses of a series of confocal images using COMSTAT2 analysis

software. Error bars represent standard deviations from biological triplicates. Student's t-test: *$P < 0.05$ and **$P < 0.01$.

726 **Figure 6**

727

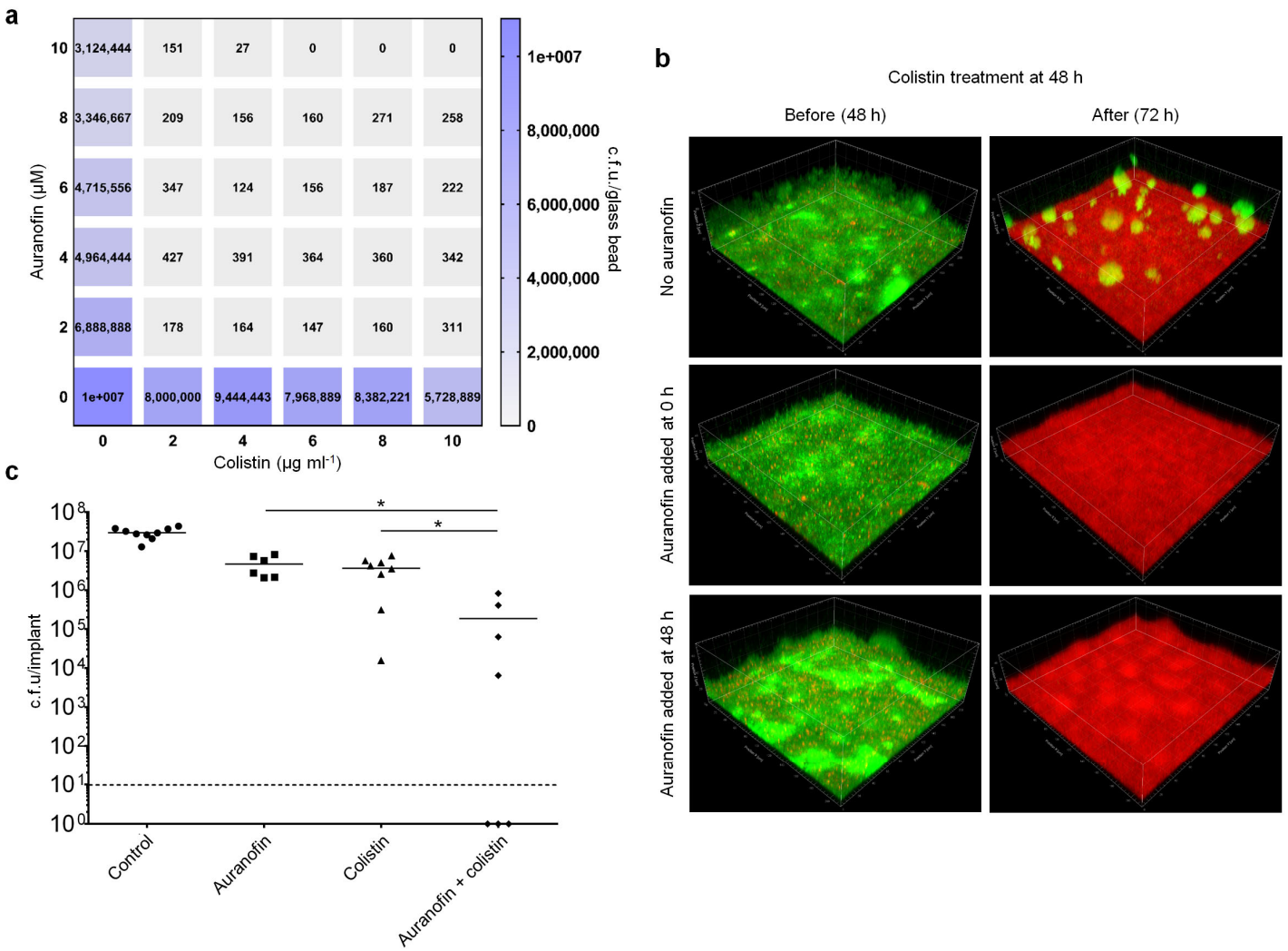

728 **Figure 6.** Auranofin displays strong synergy in eradicating *P. aeruginosa* biofilms when used
729 in combination with colistin. (a) Mean c.f.u of cells isolated from one-day old PAO1 biofilms
730 grown on glass beads before and after treatment with indicated combinations of auranofin
731 and/or colistin in a checkerboard format. (b) Confocal fluorescence microscopy images of two-
732 day old PAO1-*gfp* flow chamber biofilms before and after treatment with 10 μg ml^{-1} colistin.
733 Auranofin (1 μM) was not added (top panels), added prior to biofilm formation (middle panels),
734 or added together with colistin (bottom panels). Dead cells were revealed by staining with
735 propidium iodide. (c) Mean c.f.u per implant of *in vivo* PAO1 biofilms obtained from silicone
736 implants in the peritoneal space of mice, treated with auranofin (10 μM), colistin (1 mg kg^{-1})
737 or a combination of both drugs. Dotted horizontal lines represent limit of detection. Mann-
738 Whitney test: $*P < 0.01$.